

# Understanding visual map formation through vortex dynamics of spin Hamiltonian models

Myoung Won Cho\* and Seunghwan Kim†

*Department of Physics,  
Pohang University of Science and Technology,  
Kyungpook, Pohang, 790-794, South Korea*

(Dated: May 22, 2019)

We introduce a general method for cerebral cortical map generation and apply it to pattern formation in orientation and ocular dominance columns of the brain. From a known cortical structure, we build spin Hamiltonian models with long-range interactions of the Mexican hat type. These Hamiltonian models allow a coherent interpretation of the diverse phenomena in the map formation in the visual cortex with the help of relaxation dynamics of spins. In particular, we predict various phenomena of self-organization in orientation and ocular map formation including the pinwheel annihilation and its dependency on the columnar wave vector and boundary conditions.

PACS numbers: 42.66.-p, 87.10.+e, 75.10.Hk, 89.75.Fb

A series of experiments suggest that important elements of the organization of ocular dominance (OD) and orientation preference (OP) maps in the striate cortex are not prespecified but emergent during an activity-driven, self-organizing process [1, 2, 3, 4]. An optical imaging technique [5, 6, 7] revealed the detailed maps of OD and OP over small patches of the cortex, which prompted several methods for the map generation and various attempts for the analysis of the properties of the emerging patterns [8]. In this paper, we propose a non-competitive Hebbian model, called the fibre bundle map (FBM) method, which is closely related to problems in statistical mechanics. The map formation of OP and OD columns are explained with the help of the simple spin Hamiltonians using this method. The statistical analysis of these spin Hamiltonians leads to the successful prediction of several properties of self-organized patterns that have been observed in experiments and numerical simulations.

In the OP columnar patterns, there are two prominent experimentally observed features: (1) singular points (so called “pinwheels”) are point-like discontinuities around which the orientation preference changes by multiples of  $180^\circ$  along a closed loop, and (2) linear zones are regions where iso-orientation domains (IODs) are straight and run in parallel for a considerable distance [9, 10, 11]. In the analysis of competitive Hebbian models [12, 13], the bifurcation points between homogeneous and inhomogeneous solutions and the change of the wavelength  $\Lambda$  in OP or OD columns are predicted [14, 15, 16]. Such linear zones in the OP pattern or the OD segregations are the major features of inhomogeneous states. Some experimental or simulational results suggest that pinwheels are not permanent structures but can be annihilated in the course of active-dependent development [17]. The perpendicular tendency of IODs and bands of OD with the margin of the striate cortex is also reported [18, 19]. There are some evidence that OP and OD columns are

not independent but correlated. Pinwheels have a tendency to align with the centers of OD bands and IODs intersect the borders of OD bands at a steep angle [18]. The influence of the interactions between OP and OD columns on the pinwheel stability was also predicted [17].

In our spin analogy, the progress in the visual map formation corresponds to the relaxation dynamics of the classical spin models, where the pinwheels in orientation maps can be regarded as spin vortices. In this context, the pinwheel instability and its annihilation rate can be predicted from the free energy of the topological excitation or the Kosterlitz and Thouless transition temperature. We will show that there is a bifurcation point between the homogeneous and inhomogeneous states depending on the strength of the relative inhibitory activity  $k$  in lateral currents in the cortex. It is similar to the role of the cooperation range  $\sigma$  in competitive Hebbian models [14, 15, 16]. Our model allows the calculation of the columnar wavelength and the correlation function. The extension of our model to the  $O(3)$  or the Heisenberg model allows the correlation between the OP and OD columns, which predicts the orthogonal property between IODs and the borders of OD bands, and the influence of strong OD segregations on the pinwheel stability. Another orthogonal property of patterns in area boundaries can be derived from the equilibrium condition.

The six layers in the neocortex can be classified into three different functional types. The layer IV neurons first get the long range input signals and send them up vertically to layer II and III that are called the true association cortex. Output signals are sent down to the layer V and VI, and sent further to the thalamus or other deep and distant neural structures. Horizontal connections also happen in the superficial (layer II and III) pyramidal neurons and have usual antagonistic propensity which sharpens responsiveness to an area. However, the superficial pyramidal neurons also send excitatory recurrent to adjacent neurons due to unmyelinated collaterals.

Horizontal or lateral connections have such distance dependent (so called "Mexican hat" shaped) excitatory or inhibitory activity. Some bunches of neurons also make columnar clusters called minicolumns and such aggregations are needed considering more faculty or higher dimensional property of processing elements [21, 22].

Now our FBM model starts from the assumption that the total space  $E$  is composed by lattice (or base) space  $B$  and pattern (or fibre) space  $F$ , and *the pattern space does not take part in the decision of "stimulus receptor* (which means the winner neuron in Kohonen's self-organizing feature map method [23])" differenting with the lattice space. There needs also a transition function group  $G$  (called a structure group) of a homeomorphism of the fibre space  $F$  to describe what happens if "excitatory" or "inhibitory" activate each other. Sometimes the fibre group  $F$  is replaced by the structure group  $G$ , which deserves to be called symmetry (or gauge) group. If there is no anisotropic connections, the pattern formation will be determined just by neighborhood interactions and random external stimuli.

Now in the case of OP map formation, the patterns are defined by the phase angles  $\phi_i$  ( $0 \leq \phi_i < \pi$ ). If there are driven force by horizontal currents and external stimuli, the changes of phases are described such that

$$\frac{\partial \phi_i}{\partial t} = -\frac{\partial H}{\partial \phi_i} = -2\varepsilon \sum_j I(\vec{r}_i, \vec{r}_j) \sin(2\phi_i - 2\phi_j) - 2\mu B_i \sin(2\phi_i - 2\phi'_i), \quad (1)$$

where  $\varepsilon$  and  $\mu$  are the relative activity rate by horizontal connections and external stimuli.  $B$  and  $\phi'$  are the strength and the phase of external stimulus. We use the neighborhood interaction function  $I$  such as

$$I_{WL}(\vec{r}_i, \vec{r}_j) = \left(1 - k \frac{|\vec{r}_i - \vec{r}_j|^2}{\sigma^2}\right) \exp\left(-\frac{|\vec{r}_i - \vec{r}_j|^2}{2\sigma^2}\right) \quad (2)$$

(there is also another well-known Mexican hat shaped function,  $I_{DOG}(r) = \exp(-r^2/2\sigma_1^2) - k \exp(-r^2/2\sigma_2^2)$ , called difference of Gaussians (DOG) filter). The corresponding Hamiltonian of Eq. (1) is rewritten as the spin Hamiltonian

$$H = -\sum_{i,j} J(\vec{r}_i, \vec{r}_j) \mathbf{S}_i \cdot \mathbf{S}_j - \sum_i \mathbf{h}_i \cdot \mathbf{S}_i, \quad (3)$$

where  $J(\vec{r}_i, \vec{r}_j) = \frac{\varepsilon}{2} I(\vec{r}_i, \vec{r}_j)$  is a site distance dependent interaction energy. The site states  $\mathbf{S}_i = (\cos 2\phi_i, \sin 2\phi_i)$  and the external stimuli  $\mathbf{h}_i = (\mu B_i \cos 2\phi'_i, \mu B_i \sin 2\phi'_i)$  are 2-component vectors. In the case of OD maps,  $\mathbf{S}_i$  are 1-component with  $\pm 1$  values such as the Ising model. Our spin Hamiltonian with long-range interactions have been studied in the context of both XY and Ising models with most interactions in the form of  $J(r) \sim r^{-\alpha}$  [24, 25, 26, 27].

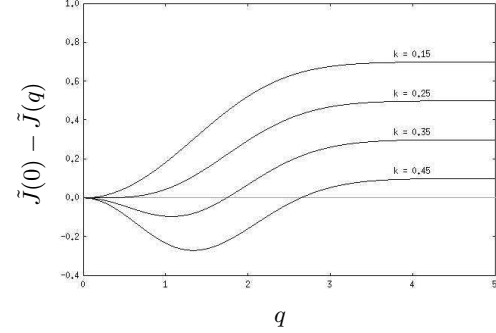


FIG. 1: The plot of  $\tilde{J}(0) - \tilde{J}(q)$  vs  $q$  in Eq. (5) ( $\varepsilon = 1/\pi$ ,  $\sigma = a$ ). For  $k > k_c$  ( $=1/4$ ), the minimum point at  $q^* = 0$  becomes unstable.

This Hamiltonian is easily diagonalized in the momentum space:

$$H = -\sum_{\vec{q}} \tilde{J}(\vec{q}) \mathbf{S}_{\vec{q}} \cdot \mathbf{S}_{-\vec{q}} - \sum_{\vec{q}} \mathbf{h}_{\vec{q}} \cdot \mathbf{S}_{-\vec{q}}, \quad (4)$$

where  $\tilde{J}(\vec{q}) = \sum_{\vec{r}} J(\vec{r}) e^{-i\vec{q} \cdot \vec{r}}$ ,  $\mathbf{S}_{\vec{q}} = \frac{1}{\sqrt{N}} \sum_i \mathbf{S}_i e^{-i\vec{q} \cdot \vec{r}_i}$  and  $\mathbf{h}_{\vec{q}} = \frac{1}{\sqrt{N}} \sum_i \mathbf{h}_i e^{-i\vec{q} \cdot \vec{r}_i}$ . We assume neurons do not choose or compete for their input patterns, so that the external stimuli term is regarded to be averaged out without thermal fluctuation effect. In the continuum limit, we obtain

$$\tilde{J}(\vec{q}) \simeq \pi \varepsilon \frac{\sigma^2}{a^2} (1 - 2k + k\sigma^2 q^2) e^{-\sigma^2 q^2/2}, \quad (5)$$

where  $a$  is the lattice constant.  $\tilde{J}(\vec{q})$  has the maximum at  $q^* = 0$  for  $k < k_c$  ( $=1/4$ ) and at  $q^* = \frac{1}{\sigma} \sqrt{4 - 1/k}$  for  $k > k_c$  (Fig. 1). This means that there is a threshold depending on  $k_c$  below which linear zones in OP columns or OD segregation are absent. Above the bifurcation point, linear zones or OD bands emerge with the wavelength  $\Lambda = 2\pi/q^*$ , which decreases as  $k$  increases (Fig. 2 (b) & (c)).

For the moment, the thermal effect or the interactions with OD columns are not considered. In this case, pinwheel structures cannot avoid the destiny of annihilation due to the diagonalized Hamiltonian in momentum space. In the evolutions of the OP map starting from a random state by Eq. (1), dense pinwheels first emerge with the spin-waves for  $k < k_c$  (Fig. 2 (a)) as for the classical XY model. Then pinwheels start to annihilate in pairs and eventually the map approaches a homogeneous state. For  $k > k_c$  (Fig. 2 (b)&(c)), pinwheels emerge with the plane-waves (linear zones) and are annihilated in time as well. The OP map will eventually approach the equilibrium state that is composed of a uni-directional plane-wave, the winner in the competition among  $|\vec{q}| = q^*$  states.

By using the parabolic behavior of  $-\tilde{J}(q)$  near the min-

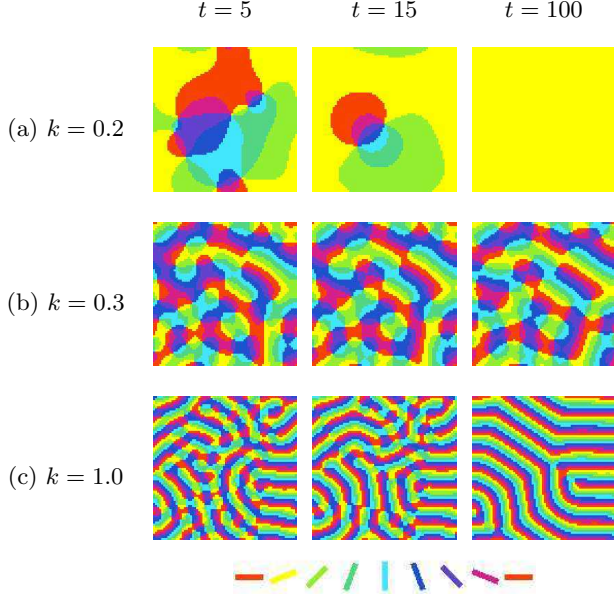


FIG. 2: Simulation results of the OP map using Eq. (1). Maps are generated with  $\sigma^2 = 6$ ,  $\varepsilon = 10^{-3}$ ,  $\mu = 0$  (zero temperature), periodic boundary condition and an initially random state in  $70 \times 70$  lattice.

imum point  $q^*$ , the Hamiltonian can be approximated as

$$H \simeq - \sum_{\vec{q}} \left[ \tilde{J}(q^*) + \frac{1}{2} \tilde{J}''(q^*)(q - q^*)^2 \right] \mathbf{S}_{\vec{q}} \cdot \mathbf{S}_{-\vec{q}} \quad (6)$$

or the effective Hamiltonian depending on the phase is given by

$$H[\phi] \simeq -N J_s + \frac{J_p}{2} \int d\vec{r} |2\vec{\nabla}\phi - \vec{q}^*|^2, \quad (7)$$

where  $J_s = \tilde{J}(q^*)$ ,  $J_p = -\tilde{J}''(q^*)/a^2$  ( $= 2\pi\varepsilon\frac{\sigma^4}{a^4}(4k-1)\exp(-2+1/2k)$  for  $k > k_c$ ), and both  $J_s$  and  $J_p$  are positive for all  $k$ . The second term in Eq. (7) describes the low energy excitation by pinwheel formation. Here, the term with  $q^*$  for plane-wave solutions do not contribute in the pinwheel formation energy since  $\nabla \times \nabla\phi_{pw} = 0$  and the line integral around any contour vanish also by Stoke's theorem. Just adapting the results in vortex dynamics, we can obtain the change in free energy due to the formation of a pinwheel,  $\Delta G = (\pi J_p - 2k_B T) \ln(L/a)$ , and the phase transition temperature,  $T_{KT} = \pi J_p / 2k_B$ .

The visual cortex arises through activity-dependent refinement of initially unselective patterns of synaptic connections, whereas dense pinwheels emerge when orientation selectivity is first established and the density of pinwheels decreases by annihilations in time. The observed pinwheel densities differ in several species and such difference in the pinwheel annihilation rates is discussed by Wolf *et al.* [17]. Now we can predict the relative pinwheel annihilation rates in terms of  $\Delta G$  or  $T_{KT}$ : (i) As  $k$  increases for  $k > k_c$ ,  $J_p$  increases and

the pinwheels become more unstable. For same  $\varepsilon$  and  $\sigma$ ,  $\Lambda$  decreases as  $k$  increases and the system with a narrower wavelength relaxes to the equilibrium state more rapidly (Fig. 2 (b) & (c)). (ii) As  $\sigma$  increase, pinwheels are more unstable. But  $\Lambda$  is proportional to  $\sigma$ , and the system with a narrower wavelength relaxes to the equilibrium state more slowly in this case. (iii) The annihilation rate increases for larger synapse plasticity or a learning rate  $\varepsilon$ . (iv) Thermal fluctuations may lead to the persistence of the pinwheel structure but they also disturb the map organization. (v) The interaction energy of a pair of pinwheel-antipinwheel is  $E_{pair}(\vec{r}_1, \vec{r}_2) = -2\pi J_p \ln(|\vec{r}_1 - \vec{r}_2|/a)$ . But there is a pinwheel annihilation mechanism by collisions not only between opposite chirality but also with area boundaries. The probability of collision with area boundaries decreases as the lattice becomes larger for random moving pinwheels. (vi) To include the interactions between OD and OP columns, our model has to be extended to the  $O(3)$  symmetry or Heisenberg model. The classical anisotropic Heisenberg model is described by

$$H = -K \sum_{\langle ij \rangle} (S_i^x S_j^x + S_i^y S_j^y + \lambda S_i^z S_j^z), \quad (8)$$

where  $K > 0$ . This model predicts that  $T_{KT}$  approaches 0 as  $\lambda$  approaches 1 [28]. This result can be translated as follows: the pinwheel structures last longer or even become stabilized in the presence of strong OD column influences or segregations.

The extension to the Heisenberg model also explains the orthogonal property between the borders of OD bands and the IODs that are experimentally observed. Let us consider the gradient or normal vectors of IODs at  $S_x = 0$  and  $S_y = 0$ . These two vectors intersect perpendicularly at pinwheels. The borders of the opposite ocular dominance domains can be represented as  $S_z = 0$ , which will meet also perpendicularly with other contours,  $S_x = 0$  or  $S_y = 0$ . Therefore, the borders of opposite ocular dominance domains are mathematically equivalent to iso-orientation contours and intersect perpendicularly

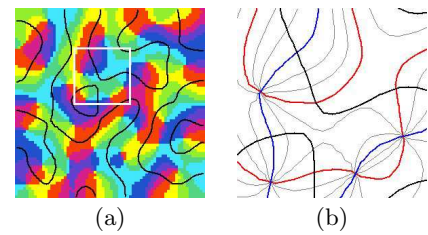


FIG. 3: (a) An simulation result of OP and OD columnar patterns using Eq. (3) with  $\mathbf{S} = (S_x, S_y, S_z)$  and (b) its detailed contour feature in a white rectangle. The blue lines correspond to  $S_x = 0$  ( $\phi = \frac{\pi}{4}$  or  $\frac{3\pi}{4}$ ) domains and the red lines,  $S_y = 0$  ( $\phi = 0$  or  $\frac{\pi}{2}$ ) domains. The black lines are the borders of opposite ocular dominance (or  $S_z = 0$  domains) in both figures.

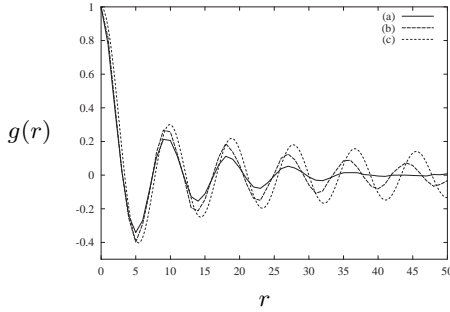


FIG. 4: (a) Normalized autocorrelation function  $g(r)$  of the simulation results in Fig. 2 (c) at  $t = 5$  and (b)  $t = 100$ . (c) The zeroth Bessel function  $J_0(q^*r)$ .

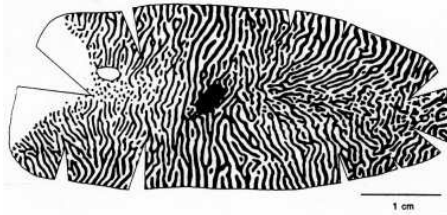


FIG. 5: The complete pattern of OD stripes in the striate cortex of a macaque monkey. There is a strong tendency for the stripes to meet the margin of striate cortex at steep or right angles (LeVay, 1985 [19]).

with each other (Fig. 3).

The correlation function for spins can be obtained from Eq. (7) as

$$\langle \mathbf{S}(r) \cdot \mathbf{S}(0) \rangle = g(r) \simeq J_0(q^*r) \left( \frac{r}{a} \right)^{-\eta(T)}, \quad (9)$$

where  $\eta(T) = k_B T / 2\pi J_p$  and  $J_0$  the zeroth Bessel function that is the correlation function of the single directional plane wave state. As map relaxes to the equilibrium state, the correlation function approaches the distribution in Eq. (9) (Fig. 4).

The perpendicular tendency with the margin of the striate cortex is attributable to the similarity between the gradient of the phase  $\nabla\phi$  and the magnetic field with  $\nabla^2\phi \sim 0$  derived from the equilibrium condition  $\delta H/\delta\phi = 0$ . The normal component of  $\nabla\phi$  vanishes at area boundaries from this condition. This is consistent with the experimental (Fig. 5) and simulational results.

Considering the complicated structures of the striate cortex, other map development schemes are possible. At the moment, however, we implemented the self-organizing map formation of OP and OD columnar patterns by focusing only on the neighborhood lateral interactions. We believe the detailed structure of receptive fields or the scatter in the topographic projection from retina to cortical locations are not essential ingredients in the cortical map organization. The structure group  $G$  in our model is more useful representation than the feature vectors  $F$ . It focuses on the transformations by the

reciprocal interactions rather than the detailed elemental informations. In the presence of OP and OD map correlations,  $G = O(3)$  rather than  $O(2) \times Z_2$  and such group representation reveals directly the interactions between different columns. The comprehensive understanding of distance dependent anisotropic Heisenberg models is not easy problem by itself and also remains as an important issue in condense matter physics, the study of which will have important implications in understanding the influences of the interactions between OD and OP columns in the cortical map formation.

\* Electronic address: mwcho@postech.edu

† Electronic address: swan@postech.edu

- [1] D. Hubel and T. N. Wiesel, *J. Physiol. (London)* **206**, 419 (1970).
- [2] D. Hubel and T. N. Wiesel, *Proc. Roy. Soc. (London) B* **278**, 377 (1977).
- [3] S. LeVay, M. Stryker, and C. Shatz, *J. Comp. Neurol.* **179**, 223 (1978).
- [4] M. P. Stryker, H. Sherk, A. G. Leventhal, and H. V. B. Hirsch, *J. Neurophysiol.* **41**, 896 (1978).
- [5] G. G. Blasdel, *J. Neurosci.* **12**, 3115 (1992).
- [6] G. G. Blasdel and G. Salama, *Nature (London)* **321**, 579 (1986).
- [7] A. Grinvald, E. Lieke, R. P. Frostig, C. Gilbert, and T. Wiesel, *Nature (London)* **324**, 361 (1986).
- [8] E. Erwin, K. Obermayer, and K. Schulten, *Neural comput.* **7**, 425 (1995).
- [9] N. V. Swindale, J. A. Matsubara, and M. S. Cynader, *J. Neurosci.* **7**, 1414 (1987).
- [10] T. Bonhoeffer and A. Grinvald, *Nature* **353**, 429 (1991).
- [11] P. E. Maldonado, I. Gödecke, C. M. Gray, and T. Bonhoeffer, *Science* **276**, 1551 (1997).
- [12] K. Obermayer, G. G. Blasdel, and K. Schulten, *Phys. Rev. A* **45**, 7568 (1992).
- [13] R. Durbin and G. Mitchison, *Nature (London)* **343**, 341 (1990).
- [14] O. Scherf, K. Pawelzik, F. Wolf, and T. Geisel, *Phys. Rev. E* **59**, 6977 (1999).
- [15] G. J. Goodhill and A. Cimponeriu, *Network: Comput. Neural Syst.* **11**, 153 (2000).
- [16] F. Hoffmüller, F. Wolf, and T. Geisel, *Neurol. Conf.* **1**, 97 (1995).
- [17] F. Wolf and T. Geisel, *Nature* **395**, 73 (1998).
- [18] K. Obermayer and G. G. Blasdel, *J. Neurosci.* **13**, 4114 (1993).
- [19] S. LeVay, D. H. Connolly, J. Houde, and D. C. V. Essen, *J. Neurosci.* **5**, 486 (1985).
- [20] J. M. Kosterlitz and D. J. Thouless, *J. Phys. C* **6**, 1181 (1973).
- [21] W. H. Calvin, in *The handbook of brain theory and neural networks*, edited by M. A. Arbib (MIT Press, 1998), pp. 269–272.
- [22] J. S. Lund, Q. Wu, and J. B. Levitt, in *The handbook of brain theory and neural networks*, edited by M. A. Arbib (MIT Press, 1998), pp. 1016–1021.
- [23] T. Kohonen, *Self-organization and associative memory* (Springer-Verlag, 1984).

- [24] J. L. Monroe, R. Lucente, and J. P. Hourlland, *J. Phys. A* **23**, 2555 (1990).
- [25] M. Krech and E. Luijten, *Phys. Rev. E* **61**, 2058 (2000).
- [26] M. Ifti, Q. Li, C. M. Soukoulis, and M. J. Velgakis, *Mod. Phys. Lett. B* **15**, 895 (2001).
- [27] E. Luijten and H. W. J. Blöte, *Phys. Rev. B* **56**, 8545 (1997).
- [28] S. Hikami and T. Tsuneto, *Prog. Theor. Phys.* **63**, 387 (1980).